

# Electrodynamic response of current-biased elementary cubic networks of Josephson junctions

R. De Luca and F. Romeo

*INFN and DIIMA, University of Salerno, I-84084 Fisciano, Salerno, Italy*

(Received 4 January 2002; revised manuscript received 7 March 2002; published 3 July 2002)

We study the electrodynamic behavior of elementary cubic networks of Josephson junctions in the presence of a constant current bias and of a uniform external magnetic field. We find that, for well defined external field directions, the observable electrodynamic quantities, such as the time-averaged voltage  $\langle v \rangle$ , are periodic with respect to the applied flux  $\Phi_{\text{ex}}$ . Considering linear and shear strain of the network, by first order perturbation analysis on the deformation parameters it is shown that the  $\langle v \rangle$  vs  $\Phi_{\text{ex}}$  curves are still periodic. However, both periodicity and the field directions for which periodic behavior occurs differ from those found in the nondeformed case.

DOI: 10.1103/PhysRevB.66.024509

PACS number(s): 74.50.+r, 85.25.-j

## I. INTRODUCTION

Three-dimensional (3D) Josephson junction networks (JJN's) have been adopted as models of both superconducting granular systems<sup>1-9</sup> and superconductive devices.<sup>10-14</sup> Lately, 3D JJN's have been considered as circuit models of ultrasensitive magnetic field sensors.<sup>15-17</sup> Even though a great amount of experimental work has been performed on granular samples and traditional devices, 3D systems are yet to be fabricated and tested due to the inherent difficulty in patterning superconducting material in three dimensions. However, these same systems show peculiar and interesting properties,<sup>18</sup> so that it is useful to develop a full understanding of their electrodynamic response. In addition, these studies might trigger future experimental work on the subject.

An elementary cubic network of Josephson junctions is formed by twelve Josephson junctions located at the midpoints of the edges of a cubic superconducting structure, as shown in Fig. 1. When a bias current  $I_B$  is injected into the network, a so-called 3D SQUID is obtained.<sup>17</sup> This term is justified by the fact that the system behaves very similar to a dc SQUID (Refs. 10 and 11) for fields applied along the coordinate axes. Moreover, since the electrodynamic response of these models depends upon the field direction in a predictable way, it has been hypothesized that the corresponding devices might find application as ultrasensitive vectorial magnetic field sensors.<sup>15,16</sup>

In the present work we focus our attention on the presence of periodicity in the electrodynamic quantities, such as the time-averaged voltage  $\langle v \rangle$  across the twelve branches in the network, with respect to the applied magnetic flux  $\Phi_{\text{ex}}$ . Therefore, in the following section we write the time-evolution equations for the superconducting phase differences across the twelve Josephson junctions (JJ's) in the network and define the observable electrodynamic quantities of the system. In the third section we determine, by means of an analytic procedure, the field directions for which periodicity in the  $\langle v \rangle$  vs  $\Phi_{\text{ex}}$  curves is present. In the fourth section we study how the periodicity is affected by linear and shear strain of the network. Conclusions are drawn in the last section.

## II. ELECTRODYNAMICS

The electrodynamic response of 3D JJN's can be studied by solving the set of dynamical equations for the vector  $\varphi$ , whose components are the gauge-invariant superconducting phase difference  $\varphi_{\xi}(\vec{r}, t)$  across the twelve junctions in the network. In labeling the quantities  $\varphi_{\xi}(\vec{r}, t)$ , we adopt an index  $\xi$  for denoting the direction in which the junction lies ( $\xi = x, y, z$ ) and a second index  $\vec{r}$  to distinguish between the four JJ's lying in the same direction, but occupying different positions in space. By adopting the resistively shunted junction (RSJ) model,<sup>10</sup> the dynamical equations for the vector  $\varphi$  can be shown to be written as follows:<sup>18</sup>

$$\frac{d}{d\tau} \varphi + \sin \varphi + \frac{1}{2\pi\beta} \mathbf{A} \varphi = \mathbf{f}, \quad (1)$$

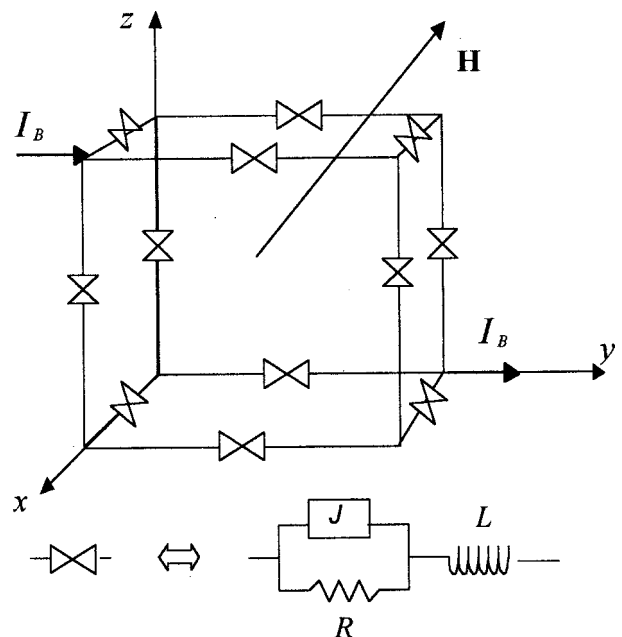


FIG. 1. Elementary cubic network of Josephson junctions. The double triangles are representative of one JJ and an inductor, as shown in the inset.

where  $\tau \equiv (2\pi R I_{J0} / \Phi_0) t$  is the normalized time variable, with  $R$  and  $I_{J0}$  the resistive junction parameter and the maximum Josephson current, respectively,  $\mathbf{A}$  is a singular  $12 \times 12$  matrix,  $\beta = L I_{J0} / \Phi_0$ ,  $L$  being the self-inductance of a single branch, and where  $\mathbf{f}$  is the forcing vector which includes both the bias current and the external magnetic field. In Eq. (1) the matrix  $\mathbf{A}$  takes into account both the electromagnetic and the quantum mechanical coupling of the JJ's. Details on the derivation of Eq. (1) can be found in Ref. 18. We finally notice the particular notation used in Eq. (1), in which the  $\sin \varphi$  term symbolically represents a vector whose twelve components are the quantities  $\sin \varphi_{\xi}(\vec{r}, \tau)$ .

Because of the Josephson equations, the branch current vector  $\mathbf{i}$ , whose components are normalized with respect to the maximum Josephson current  $I_{J0}$ , may be defined as follows:

$$\mathbf{i} = \mathbf{f} - \frac{1}{2\pi\beta} \mathbf{A} \varphi. \quad (2)$$

If we assume that the forcing term is constant, the voltage vector, normalized with respect to  $R I_{J0}$ , can be written as follows:

$$\mathbf{v}(\tau) = \frac{d}{d\tau} \varphi + 2\pi\beta \frac{d}{d\tau} \mathbf{i} = (1 - \mathbf{A}) \frac{d}{d\tau} \varphi. \quad (3)$$

The components of the current vector  $\mathbf{i}$  and of the voltage vector  $\mathbf{v}$  are seen to be periodic with a global period  $T$ . The presence of a global period  $T$  in the electrodynamic quantities is a consequence of the properties of the matrix  $\mathbf{A}$ . Indeed, by imposing periodicity in time of the instantaneous current vector  $\mathbf{i}$ , we may write

$$\mathbf{A} \varphi(\tau + T) = \mathbf{A} \varphi(\tau). \quad (4)$$

We can argue, by analogy with the single JJ case, that some junctions in the network undergo a  $2\pi$  phase shift after a time  $T$  for values of the bias current greater than some critical current value  $I_c$ . As in the SQUID,  $I_c$  depends on the external magnetic field amplitude, but, in contrast to what happens in the planar case, it also depends upon the direction of the external magnetic field. By following the analogy with the single JJ case, then, we can set

$$\varphi(\tau + T) = \varphi(\tau) + 2\pi \mathbf{K}, \quad (5)$$

where  $\mathbf{K}$  is a vector whose components are either 0 or  $\pm 1$ . By substituting in Eq. (4) the expression for  $\varphi(\tau + T)$  given in Eq. (5), we get

$$\mathbf{A} \cdot \mathbf{K} = 0, \quad (6)$$

so that  $\mathbf{K}$  must belong to the null-space of the matrix  $\mathbf{A}$ . Now, since  $\mathbf{A}$  is a singular matrix, its null-space is nontrivial; this ensures that not all the components of  $\mathbf{K}$  are necessarily null when some of the junctions in the network are in the resistive state. Naturally, the solution  $\mathbf{K} = 0$  to Eq. (6) corresponds to the zero-voltage state of the system.

In order to illustrate this point more clearly, let us refer to a planar dc SQUID. In this case the matrix  $\mathbf{A}$ , which may be denoted as  $\mathbf{A}_{\text{SQUID}}$ , is given by<sup>19</sup>

$$\mathbf{A}_{\text{SQUID}} = \begin{pmatrix} -1 & +1 \\ +1 & -1 \end{pmatrix}. \quad (7)$$

The dynamical equations for the superconducting phase differences of the two JJ's in the SQUID is formally identical to Eq. (1). Since the matrix  $\mathbf{A}_{\text{SQUID}}$  is singular, the null space of the matrix itself can be seen to be nonempty, so that from Eq. (1) we can argue that the time derivative of the vector  $\varphi$  is invariant for a translation  $T$  in time, if  $\mathbf{K}$  belongs to the null space of  $\mathbf{A}$ . In this case the vector  $\mathbf{K}$  can be written as follows:

$$\mathbf{K} = \begin{pmatrix} 1 \\ 1 \end{pmatrix}. \quad (8)$$

This means that the two identical JJ's in a SQUID are in phase when a dissipative dynamical state is realized under a constant external forcing term  $\mathbf{f}$ .

As for the instantaneous voltage, periodic behavior in the cubic system comes from Eq. (5), given that it is possible to write the vector  $\mathbf{v}(\tau)$  in terms of the time derivative of  $\varphi$ , as in Eq. (3). Periodicity in the voltages induces periodic behavior in the instantaneous currents. Setting  $\beta = 0.5$ ,  $I_B = 3.5 I_{J0}$ , and  $\Phi_{\text{ex}} = 0.4 \Phi_0$ , taking the field in the  $z$  direction, instantaneous voltages and currents are shown in Figs. 2(a)–2(c) and in Figs. 3(a), 3(b), respectively, where periodicity is clearly visible. Experimentally observable currents and voltages, however, are related to the time average of the corresponding instantaneous quantities. Since the instantaneous expressions of  $\mathbf{i}$  and  $\mathbf{v}$  are periodic in time, the average value of these quantities  $\langle \mathbf{i} \rangle$  and  $\langle \mathbf{v} \rangle$ , respectively, can be calculated over a single period  $T$ , if the value of  $T$  is exactly known. For more practical purposes, numerical evaluation of  $\langle \mathbf{i} \rangle$  and  $\langle \mathbf{v} \rangle$  can be performed over a rather high number of periods as follows:

$$\langle \mathbf{v} \rangle = \frac{1}{M} \int_{\tau_0}^{\tau_0 + M} \mathbf{v}(\tau) d\tau, \quad (9)$$

where  $M$  is a positive real number much greater than  $T$  and  $\tau_0$  is an arbitrary normalized time value.

### III. PERIODICITY OF THE OBSERVABLE QUANTITIES

In order to find periodicity with respect to the applied magnetic flux  $\Phi_{\text{ex}} = \mu_0 H a^2$ ,  $H$  being the external magnetic field amplitude and  $a$  the length of the cube side, the matrix  $\mathbf{A}$  and the forcing term  $\mathbf{f}$  need to be defined. Naturally, as in the SQUID case, it can be proven that no periodicity can be present with respect to the bias current  $I_B$ . Let us then start by considering the expression for the  $12 \times 12$  matrix  $\mathbf{A}$ :

$$\mathbf{A} = -L \mathbf{T} (\mathbf{M} \cdot \mathbf{T})^{-1} \mathbf{F}, \quad (10)$$

where  $\mathbf{T}$  is a  $12 \times 5$  matrix relating the twelve branch currents to only five independent currents,  $\mathbf{M}$  and  $\mathbf{F}$  are  $5 \times 12$  matrices which relate the fluxes linked to the cubic faces to

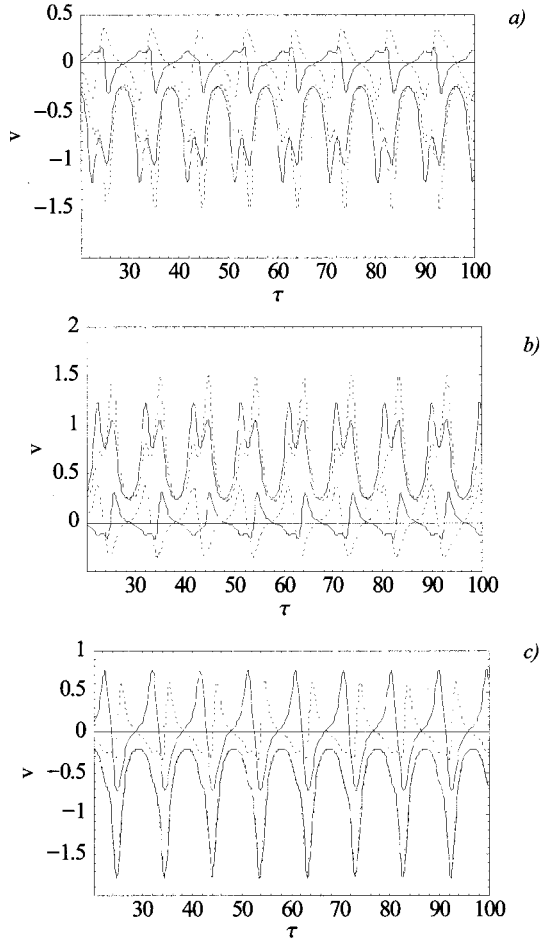


FIG. 2.  $v_\xi$  vs  $\tau$  curves for  $\beta=0.5$ ,  $i_B=3.5$ , and for applied field ( $\Psi_{\text{ext}}=0.4$ ) along the  $z$  axis. (a)  $v_x(\vec{r}, \tau)$  vs  $\tau$  curves: the instantaneous voltages  $v_x(0, \tau)$  and  $v_x(a\hat{y} + a\hat{z}, \tau)$  lie close to the zero-voltage axis and are represented, respectively, by a full and a dotted line; the voltages  $v_x(a\hat{y}, \tau)$  and  $v_x(a\hat{z}, \tau)$  are represented, respectively, by the dotted and the full lines below the axis. (b)  $v_y(\vec{r}, \tau)$  vs  $\tau$  curves: the instantaneous voltages  $v_y(a\hat{x}, \tau)$  and  $v_y(a\hat{z}, \tau)$  lie close to the zero-voltage axis and are represented, respectively, by a dotted and a full line; the voltages  $v_y(0, \tau)$  and  $v_y(a\hat{x} + a\hat{z}, \tau)$  are represented, respectively, by a full and a dotted line above the axis. (c)  $v_z(\vec{r}, \tau)$  vs  $\tau$  curves: the instantaneous voltages  $v_z(0, \tau)$  and  $v_z(a\hat{x} + a\hat{y}, \tau)$  lie close to the zero-voltage axis and are represented, respectively, by a full and a dotted line; the voltages  $v_z(a\hat{x}, \tau)$  and  $v_z(a\hat{y}, \tau)$  coincide and are represented by the curve below the  $\tau$  axis.

the branch currents and to the superconducting phase differences  $\varphi_\xi(\vec{r}, \tau)$ , respectively. A periodicity  $\mathbf{p}$  in the forcing term  $\mathbf{f}$  gives  $\langle \mathbf{v} \rangle = \langle \mathbf{v}^* \rangle$ , where  $\langle \mathbf{v}^* \rangle$  is the time-averaged value of the instantaneous voltage obtained for  $\mathbf{f}^* = \mathbf{f} + \mathbf{p}$ . In order to satisfy the relation  $\langle \mathbf{v} \rangle = \langle \mathbf{v}^* \rangle$ , by denoting with  $\varphi^*$  the solution to Eq. (1) for  $\mathbf{f}^*$ , we set

$$\langle \sin \varphi \rangle + \frac{1}{2\pi\beta} \mathbf{A} \langle \varphi \rangle = \mathbf{p} + \langle \sin \varphi^* \rangle + \frac{1}{2\pi\beta} \mathbf{A} \langle \varphi^* \rangle. \quad (11)$$

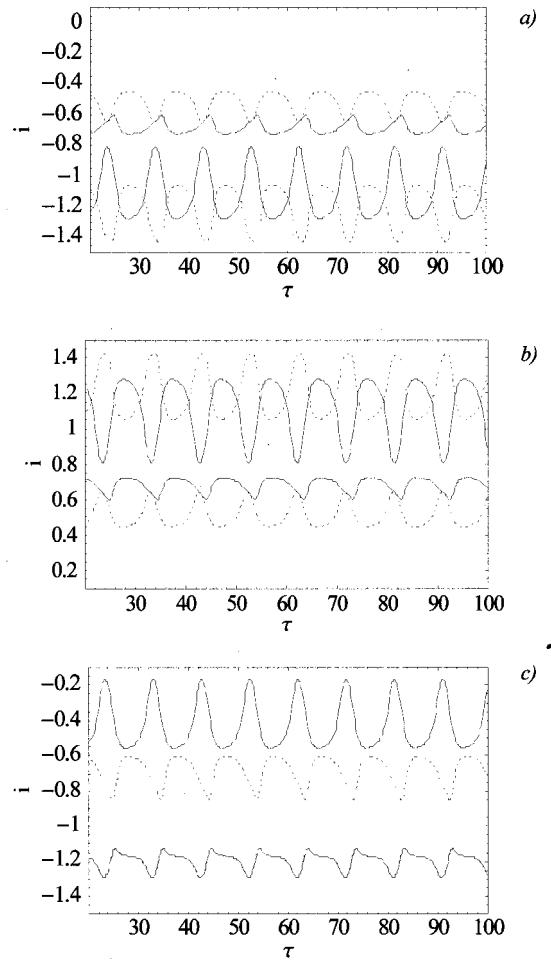


FIG. 3.  $i_\xi$  vs  $\tau$  curves for  $\beta=0.5$ ,  $i_B=3.5$ , and for applied field ( $\Psi_{\text{ext}}=0.4$ ) along the  $z$  axis. (a)  $i_x(\vec{r}, \tau)$  vs  $\tau$  curves: the instantaneous currents  $i_x(0, \tau)$  and  $i_x(a\hat{y} + a\hat{z}, \tau)$  lie close to the  $i = -0.6$  value and are represented, respectively, by a full and a dotted line; the currents  $i_x(a\hat{y}, \tau)$  and  $i_x(a\hat{z}, \tau)$  are represented, respectively, by the dotted and the full lines below the first two curves. (b)  $i_y(\vec{r}, \tau)$  vs  $\tau$  curves: the instantaneous currents  $i_y(a\hat{x}, \tau)$  and  $i_y(a\hat{z}, \tau)$  lie close to the  $i = 0.6$  value and are represented, respectively, by a dotted and a full line; the currents  $i_y(0, \tau)$  and  $i_y(a\hat{x} + a\hat{z}, \tau)$  are represented, respectively, by the full line and the dashed line above the latter couple of curves. (c)  $i_z(\vec{r}, \tau)$  vs  $\tau$  curves: the instantaneous currents  $i_z(0, \tau)$  and  $i_z(a\hat{x} + a\hat{y}, \tau)$  lie close to the  $i = -0.6$  value and are represented, respectively, by a full and a dotted line; the currents  $i_z(a\hat{x}, \tau)$  and  $i_z(a\hat{y}, \tau)$  coincide and are represented by the curve which lies close to the  $i = -1.2$  value.

By inspection we see that Eq. (11) may be satisfied by setting  $\varphi^* = \varphi + 2\pi\tilde{\mathbf{K}}$ , where  $\tilde{\mathbf{K}}$  is a vector whose components are integers. Therefore, the period  $\mathbf{p}$  can be expressed as follows:

$$\mathbf{p} = -\frac{1}{\beta} \mathbf{A} \cdot \tilde{\mathbf{K}}. \quad (12)$$

We now need to express the forcing term in its parts. By referring to Ref. 18, we get, under zero field cooling conditions,

$$\mathbf{f} = i_B(\mathbf{C} - \mathbf{1})\mathbf{V}_I + \frac{\psi_{\text{ext}}}{\beta}\mathbf{V}_\phi, \quad (13)$$

where  $\mathbf{C} = \mathbf{T}(\mathbf{M} \cdot \mathbf{T})^{-1}\mathbf{M}$ ,  $\mathbf{1}$  is the  $12 \times 12$  identity matrix,  $\mathbf{V}_I$  is a twelve-component column vector representative of the bias configuration chosen,  $\Psi_{\text{ex}} = \Phi_{\text{ex}}/\Phi_0$ ,  $i_B = I_B/I_{J0}$  and where  $\mathbf{V}_\phi = -L\mathbf{T}(\mathbf{M} \cdot \mathbf{T})^{-1}\boldsymbol{\Gamma}$ ,  $\boldsymbol{\Gamma}$  being the following vector:

$$\boldsymbol{\Gamma} = \begin{pmatrix} \hat{\mathbf{H}} \cdot \frac{\mathbf{S}_{yz}^{(0)}}{a^2} \\ \hat{\mathbf{H}} \cdot \frac{\mathbf{S}_{yz}^{(1)}}{a^2} \\ \hat{\mathbf{H}} \cdot \frac{\mathbf{S}_{zx}^{(0)}}{a^2} \\ \hat{\mathbf{H}} \cdot \frac{\mathbf{S}_{zx}^{(1)}}{a^2} \\ \hat{\mathbf{H}} \cdot \frac{\mathbf{S}_{xy}^{(0)}}{a^2} \end{pmatrix} = \begin{pmatrix} -\cos \gamma_x \\ \cos \gamma_x \\ -\cos \gamma_y \\ \cos \gamma_y \\ -\cos \gamma_z \end{pmatrix}. \quad (14)$$

The vectors  $\mathbf{S}_{\mu\nu}^{(i)}$  in Eq. (14) are the area vectors of the cubic faces lying in the  $\mu\nu$  plane, the index  $i$  being 0 if the face has one vertex in the origin, 1 otherwise. In the case of an undeformed cubic system the area vectors lie along the directions of the coordinate axes, so that the scalar product between the external field and  $\mathbf{S}_{\mu\nu}^{(i)}$  give the directional cosines  $\cos \gamma_\xi$  ( $\xi = x, y, z$ ) of the external field itself relative to the coordinate axes. In analogy to the SQUID case, where it is possible to prove that there cannot be periodicity with respect to the bias current for fixed values of the external magnetic field,<sup>10</sup> we take the period in the forcing term to be given by an increment  $\Delta\Psi_{\text{ex}}^{(0)}$  in the normalized applied flux  $\Psi_{\text{ex}}$  at a fixed value of the bias current. We thus set

$$\mathbf{p} = -\frac{\Delta\Psi_{\text{ex}}^{(0)}}{\beta}\mathbf{V}_\phi = -\frac{1}{\beta}\mathbf{A} \cdot \tilde{\mathbf{K}}. \quad (15)$$

By now expliciting the vector  $\mathbf{V}_\phi$  and the matrix  $\mathbf{A}$  in terms of their elementary components, we have

$$\mathbf{B}(\Delta\Psi_{\text{ex}}^{(0)}\boldsymbol{\Gamma} - \mathbf{F} \cdot \tilde{\mathbf{K}}) = 0, \quad (16)$$

where  $\mathbf{B} = -L\mathbf{T}(\mathbf{M} \cdot \mathbf{T})^{-1}$ . Now, since  $\mathbf{B}$  has a null space of dimension zero, we may set

$$\Delta\Psi_{\text{ex}}^{(0)}\boldsymbol{\Gamma} = \mathbf{F} \cdot \tilde{\mathbf{K}}. \quad (17)$$

Therefore, if there exist a real number  $\Delta\Psi_{\text{ex}}^{(0)}$  such that Eq. (17) is satisfied, the time-averaged voltage  $\langle v \rangle$  is periodic in  $\Psi_{\text{ex}}$ . We can extract three linearly independent relations from Eq. (17), namely,

$$\begin{aligned} \Delta\Psi_{\text{ex}}^{(0)} \cos \gamma_x &= i, \\ \Delta\Psi_{\text{ex}}^{(0)} \cos \gamma_y &= j, \end{aligned} \quad (18)$$

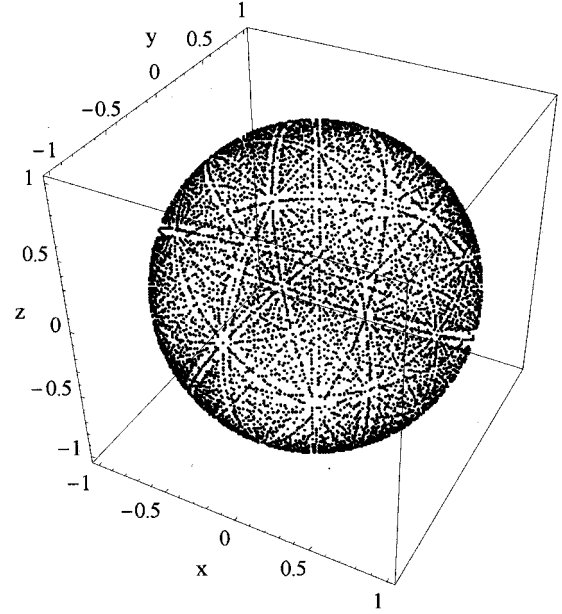


FIG. 4. Field directions for which the  $\langle v \rangle$  vs  $\Psi_{\text{ex}}$  curves of the homogeneous cubic network show periodicity. The representative points on the unitary sphere are plotted for the indices  $i, j$ , and  $k$  [Eq. (20) in the text] running from 0 to 10.

$$\Delta\Psi_{\text{ex}}^{(0)} \cos \gamma_z = k,$$

where  $i, j, k$  are integers. The possible periods can thus be written as follows:

$$\Delta\Psi_{\text{ex}}^{(0)} = \sqrt{i^2 + j^2 + k^2}, \quad (19)$$

so that the field directions  $\hat{\mathbf{H}}$ , for which periodicity is present in the  $\langle v \rangle$  vs  $\Psi_{\text{ex}}$  curves, are given by the following expression:

$$\hat{\mathbf{H}} = \frac{(i, j, k)}{\sqrt{i^2 + j^2 + k^2}}. \quad (20)$$

In Fig. 4 we represent the possible field directions for the indices  $i, j$  and  $k$  running from 0 to 10.

#### IV. STRUCTURAL DEFORMATION

In the case of slight structural deformation of the system, such as linear and shear strain [Figs. 5(a) and 5(b), respectively], we can still predict the periodicity of the  $\langle v \rangle$  vs  $\Psi_{\text{ex}}$  curves by a first-order perturbation analysis as follows.

##### A. Linear strain

Let us define the area vectors generated by elongation  $\Delta a$  of the lateral sides of the cubic network:

$$\begin{aligned} \mathbf{S}_{yz}^{(1)} &= (a + \Delta a)a\hat{\mathbf{x}}, \\ \mathbf{S}_{zx}^{(1)} &= (a + \Delta a)a\hat{\mathbf{y}}, \end{aligned} \quad (21)$$

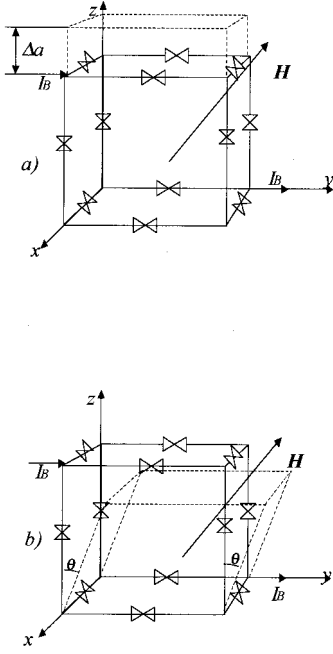


FIG. 5. Linear (a) and shear (b) strain in the network.

$$\mathbf{S}_{xy}^{(1)} = a^2 \hat{\mathbf{z}}.$$

By proceeding in the same way as in the previous section, we may consider a relation similar to Eq. (17) as a starting point. In this way, we can write the three independent relations defining the field directions for which a periodicity in the  $\langle \mathbf{v} \rangle$  vs  $\Psi_{\text{ex}}$  curves is present as follows:

$$\begin{aligned} \Delta \Psi_{\text{ex}}^{(l)} \left( 1 + \frac{\Delta a}{a} \right) \cos \gamma_x &= i, \\ \Delta \Psi_{\text{ex}}^{(l)} \left( 1 + \frac{\Delta a}{a} \right) \cos \gamma_y &= j, \\ \Delta \Psi_{\text{ex}}^{(l)} \cos \gamma_z &= k. \end{aligned} \quad (22)$$

Therefore, from Eq. (22) we can write

$$\Delta \Psi_{\text{ex}}^{(l)} = \Delta \Psi_{\text{ex}}^{(0)} (1 - \lambda \sin^2 \gamma_z), \quad (23)$$

where  $\lambda = \Delta a/a$ . In order to determine the field directions for which periodicity is allowed, by combining Eqs. (22) and (23) we find the following equation for  $\cos \gamma_z$ :

$$\lambda \cos^3 \gamma_z + (1 - \lambda) \cos \gamma_z - \frac{k}{\Delta \Psi_{\text{ex}}^{(0)}} = 0. \quad (24)$$

Notice that for  $\lambda = 0$  we obtain the result found in the undeformed case. After having solved for  $\cos \gamma_z$ , we can determine the periodicity  $\Delta \Psi_{\text{ex}}^{(l)}$  from Eq. (23), and the remaining components of the external fields, for which it is possible to detect periodicity in the  $\langle \mathbf{v} \rangle$  vs  $\Psi_{\text{ex}}$  curves, from Eq. (22). Results are shown in Figs. 6(a) and 6(b), where the possible field directions for the indices  $i, j$ , and  $k$  running from 0 to 10 are shown for  $\lambda = 0.1$  and  $\lambda = 0.2$ , respectively.

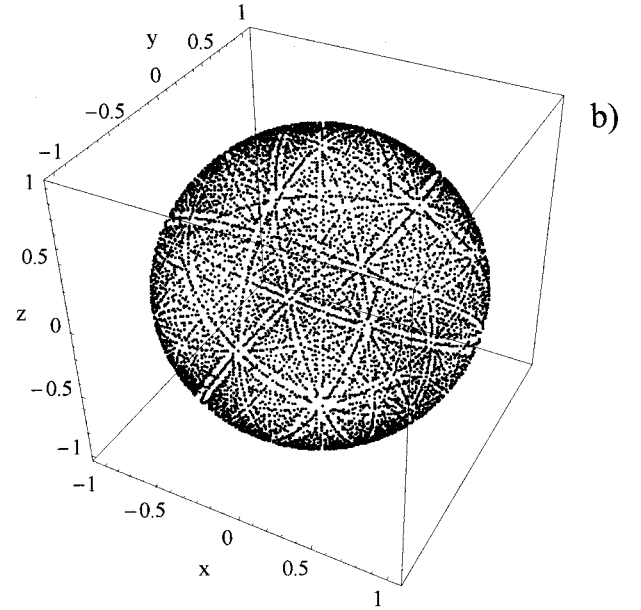
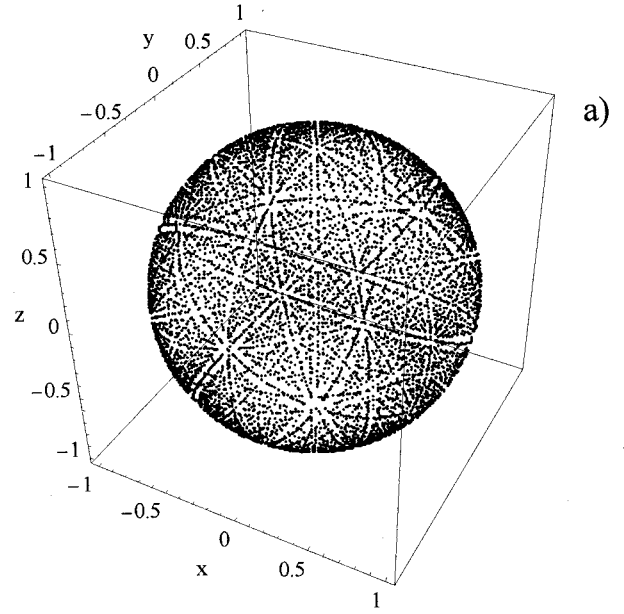


FIG. 6. Field directions for which the  $\langle v \rangle$  vs  $\Psi_{\text{ex}}$  curves of the cubic network show periodicity under the presence of linear strain. The representative points on the unitary sphere are plotted for the indices  $i, j$ , and  $k$  [Eq. (22) in the text] running from 0 to 10. (a)  $\lambda = 0.1$ ; (b)  $\lambda = 0.2$ .

### B. Shear strain

In the case of shear strain of the network, we can write the area vectors as follows:

$$\begin{aligned} \mathbf{S}_{yz}^{(1)} &= a^2 \cos \theta \hat{\mathbf{x}} \approx a^2 \hat{\mathbf{x}}, \\ \mathbf{S}_{zx}^{(1)} &= a^2 (\cos \theta \hat{\mathbf{y}} - \sin \theta \hat{\mathbf{z}}) \approx a^2 (\hat{\mathbf{y}} - \theta \hat{\mathbf{z}}), \\ \mathbf{S}_{xy}^{(1)} &= a^2 \hat{\mathbf{z}}. \end{aligned} \quad (25)$$

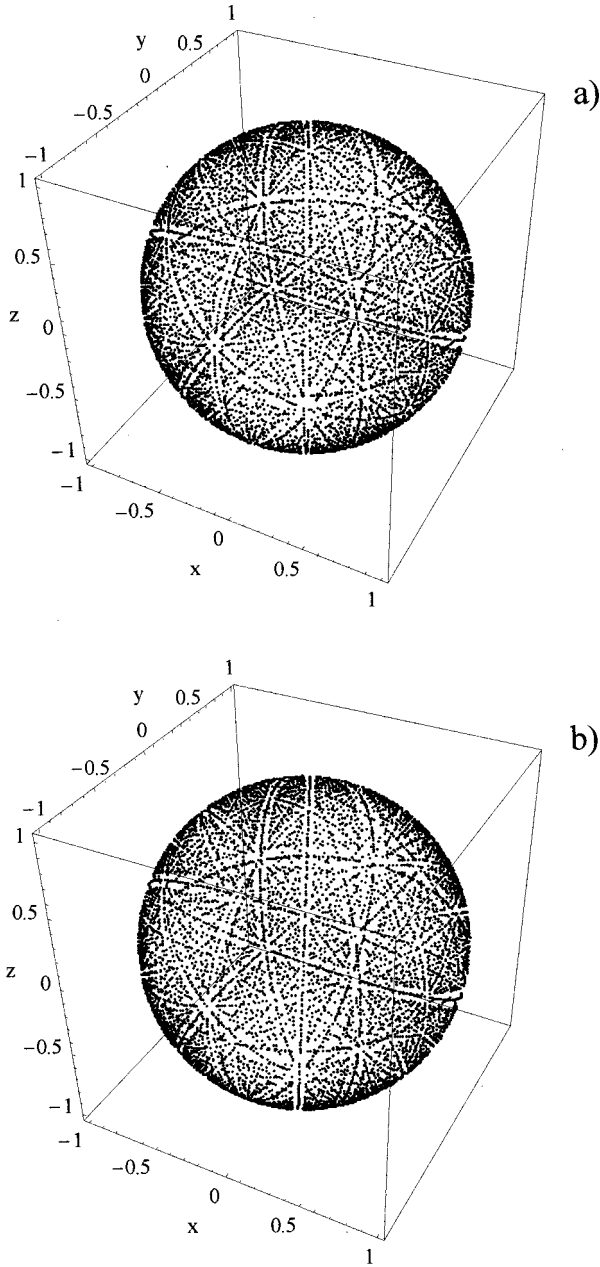


FIG. 7. Field directions for which the  $\langle v \rangle$  vs  $\Psi_{\text{ex}}$  curves of the cubic network show periodicity under the presence of shear strain. The representative points on the unitary sphere are plotted for the indices  $i$ ,  $j$ , and  $k$  [Eq. (26) in the text] running from 0 to 10. (a)  $\theta=0.01$ ; (b)  $\theta=0.1$ .

In this case the three independent relations defining the field directions for which a periodicity in the  $\langle v \rangle$  vs  $\Psi_{\text{ex}}$  curves is present are

$$\begin{aligned} \Delta\Psi_{\text{ex}}^{(s)} \cos \gamma_x &= i, \\ \Delta\Psi_{\text{ex}}^{(s)} (\cos \gamma_y - \theta \cos \gamma_z) &= j, \\ \Delta\Psi_{\text{ex}}^{(s)} \cos \gamma_z &= k. \end{aligned} \quad (26)$$

From Eq. (26) we have

$$\Delta\Psi_{\text{ex}}^{(s)} = \Delta\Psi_{\text{ex}}^{(0)} (1 + \theta \cos \gamma_y \cos \gamma_z). \quad (27)$$

We can determine the field directions for which periodicity is allowed, as it has been done in the previous subsection. By combining Eqs. (26) and (27) we find, for  $k \neq 0$ , the following equation for  $\cos \gamma_z$ :

$$\frac{j}{k} \theta \cos^3 \gamma_z + \cos \gamma_z - \frac{k}{\Delta\Psi_{\text{ex}}^{(0)}} = 0. \quad (28)$$

Notice that for  $\theta=0$  we obtain the result found in the non-deformed case. For  $k=0$ , we have  $\cos \gamma_z=0$  and the expression for  $\Delta\Psi_{\text{ex}}^{(s)}$  is found to be the same as in the unstrained case. This means that for magnetic fields in the  $x$ - $y$  plane, whose directions are the same as those allowed in the non-deformed case, no change in periodicity is detected. The value of  $\Delta\Psi_{\text{ex}}^{(s)}$  and the remaining components of the external fields for which it is possible to detect periodicity in the  $\langle v \rangle$  vs  $\Psi_{\text{ex}}$  curves can be determined from Eqs. (26) and (27). Results are shown in Figs. 7(a) and in 7(b), where the possible field directions for the indices  $i$ ,  $j$ , and  $k$  running from 0 to 10 are shown for  $\theta=0.01$  and  $\theta=0.1$ , respectively.

### C. Combined effects

Because we are only considering first-order perturbations in the deformation parameters  $\lambda$  and  $\theta$ , we can simply combine these effects in order to determine periodicity in the  $\langle v \rangle$  vs  $\Psi_{\text{ex}}$  curves and the allowed field directions in this case. We thus write

$$\begin{aligned} \Delta\Psi_{\text{ex}}^{(ls)} (1 + \lambda) \cos \gamma_x &= i, \\ \Delta\Psi_{\text{ex}}^{(ls)} (1 + \lambda) (\cos \gamma_y - \theta \cos \gamma_z) &= j, \\ \Delta\Psi_{\text{ex}}^{(ls)} \cos \gamma_z &= k, \end{aligned} \quad (29)$$

while the periodicity  $\Delta\Psi_{\text{ex}}^{(ls)}$  is determined by the following relation:

$$\Delta\Psi_{\text{ex}}^{(ls)} = \Delta\Psi_{\text{ex}}^{(0)} (1 - \lambda \sin^2 \gamma_z + \theta \cos \gamma_y \cos \gamma_z). \quad (30)$$

As before, we could determine the field directions for which periodicity is allowed, for  $k \neq 0$ , by the following equation for  $\cos \gamma_z$ :

$$\left( \lambda + \frac{j}{k} \theta \right) \cos^3 \gamma_z + (1 - \lambda) \cos \gamma_z - \frac{k}{\Delta\Psi_{\text{ex}}^{(0)}} = 0. \quad (31)$$

On the other hand, for  $k=0$ , we find the same expressions as in the case of an elongated network. Of course, we can recover the particular cases studied before by simply setting to zero the shear strain parameter  $\theta$  or the linear strain parameter  $\lambda$ .

### V. COMMENTS AND CONCLUSIONS

By an analytic approach we have proven that, in current-biased inductive cubic network of Josephson junctions, the time-averaged voltages present a periodicity  $\Delta\Psi_{\text{ex}}$  with respect to the normalized applied flux  $\Psi_{\text{ex}}$  for well defined

applied field directions. Considering linear and shear strain effects on the cubic network, a first-order perturbation analysis shows that periodic behavior of the observable electrodynamic quantities is still present for small deformations; however, periods and field directions at which periodic behavior appears are different from those found for the undeformed cubic system. These effects can be numerically evaluated. Results on the determination of field directions allowing periodicity are presented collecting points on a three-dimensional unitary sphere, each point on the sphere corresponding to one of these directions. One may notice that the collected points are distributed with different patterns on the unitary sphere, depending on the type of deformation and on the value of the deformation parameter.

This characteristic response is somehow unexpected, given the complex form of the differential equations describing the dynamics of the elementary cubic system. However, it has been shown that a straightforward analytical approach can provide a rather complete understanding of the underlying features of the model.

As for possible applications, we may notice that this net-

work may be adopted as a model system to study the magnetic response of simple eight-grain granular superconductors.<sup>20,21</sup> An artificially fabricated elementary superconducting granular system of the type considered by Busse *et al.*<sup>22</sup> should thus reveal the characteristic features investigated in the present paper. On the other hand, in a future perspective, one could also envision the use of these systems as models of 3D SQUID's. In this respect, it is important to notice that the response of mutually orthogonal planar dc SQUID's (Ref. 23) has to be corrected for mutual inductance effects between orthogonal loops. Indeed, even for fields applied to a single loop, these systems would still give signals in all channels. The symmetry properties of an hypothetical 3D SQUID, on the other hand, are such to give a SQUID-like response for fields along the coordinate axes; furthermore, mutual inductance between loops can be taken into account by means of the matrix  $\mathbf{M}$  defined in the text. We finally remark that experimental evidence needs to be gathered in such a way that the feasibility of the proposed system to be used as a vectorial magnetic field sensor may be judged also on the basis of experimental work.

- 
- <sup>1</sup>T. Wolf and A. Majhofer, Phys. Rev. B **47**, 5383 (1993).  
<sup>2</sup>J.R. Phillips, H.S.J. Van Der Zant, J. White, and T.P. Orlando, Phys. Rev. B **47**, 5219 (1993).  
<sup>3</sup>D.X. Chen, A. Sanchez, and A. Hernando, Phys. Rev. B **50**, 13 735 (1994).  
<sup>4</sup>E.A. Jagla and C.A. Balseiro, Phys. Rev. B **52**, 4494 (1995).  
<sup>5</sup>D. Dominguez and J.V. Jose, Phys. Rev. B **53**, 11 692 (1996).  
<sup>6</sup>R. De Luca, T. Di Matteo, A. Tuohimaa, and J. Paasi, Phys. Rev. B **57**, 1173 (1998).  
<sup>7</sup>T.K. Kopec and T.P. Polak, Phys. Rev. B **62**, 14 419 (2000).  
<sup>8</sup>T.K. Kopec and J.V. Jose, Phys. Rev. Lett. **84**, 749 (2000).  
<sup>9</sup>R.S. Newrock, C.J. Lobb, U. Geigenmuller, and M. Octavio, Solid State Phys. **54**, 263 (2000).  
<sup>10</sup>A. Barone and G. Paterno, *Theory and Applications of the Josephson Effect* (Wiley, New York, 1982).  
<sup>11</sup>K. K. Likharev, *Dynamics of Josephson Junctions and Circuits* (Gordon and Breach, Amsterdam, 1986).  
<sup>12</sup>P. Caputo, A.U. Ustinov, N.C.H. Lin, and S.P. Yukon, IEEE Trans. Appl. Supercond. **9**, 4538 (1999).  
<sup>13</sup>J. Oppenlaender, Ch. Haussler, and N. Schopohl, Phys. Rev. B **63**, 024511 (2001).  
<sup>14</sup>Ch. Haussler, J. Oppenlaender, and N. Schopohl, J. Appl. Phys. **89**, 1875 (2001).  
<sup>15</sup>J. Oppenlaender, Ch. Haussler, and N. Schopohl, J. Appl. Phys. **86**, 5775 (1999).  
<sup>16</sup>T. Di Matteo, R. De Luca, J. Paasi, and A. Tuohimaa, IEEE Trans. Appl. Supercond. **9**, 3515 (1999).  
<sup>17</sup>R. De Luca, T. Di Matteo, A. Tuohimaa, and J. Paasi, Philos. Mag. **80**, 897 (2000).  
<sup>18</sup>R. De Luca, Eur. Phys. J. B **22**, 139 (2001).  
<sup>19</sup>R. De Luca, Phys. Lett. A **280**, 209 (2001).  
<sup>20</sup>A. Tuohimaa, J. Paasi, T. Tarhasaari, T. Di Matteo, and R. De Luca, Phys. Rev. B **61**, 9711 (2000).  
<sup>21</sup>T. Di Matteo, A. Tuohimaa, J. Paasi, and R. De Luca, Physica C **307**, 318 (1988).  
<sup>22</sup>F. Busse, P. Seidel, M. Darula, R. Nebel, and P. Herzog, Physica C **235-240**, 3317 (1994).  
<sup>23</sup>E. Dantsker, D. Koelle, A.H. Miklich, D.T. Nemeth, F. Ludwig, J. Clarke, J.T. Longo, and V. Vinetskiy, Rev. Sci. Instrum. **65**, 3809 (1994).